Next Generation of Zinc Bisguanidine Polymerization Catalysts towards Highly Crystalline, Biodegradable Polyesters

Alina Hermann, Stephen Hill, Angela Metz, Joshua Heck, Alexander Hoffmann, Laura Hartmann,* and Sonja Herres-Pawlis*

Abstract: *Polylactide and polycaprolactone are both biodegradable polymers produced through metal-catalyzed ring-opening polymerization. For a truly sustainable lifecycle of these polymers it is essential to replace the industrially used cytotoxic catalyst tin(II) bis(2-ethylhexanoate) [Sn(Oct)$_2$] with non-toxic alternatives. Here, we report the fastest known robust catalyst in the polymerization of lactide and ε-caprolactone. This zinc guanidine catalyst can polymerize non-purified technical rac-lactide and ε-caprolactone in the melt at different [M]/[I] ratios with fast rate constants, high molar masses, and high yields in a short time, leading to colorless, transparent polymer. Moreover, we report that polylactide and polycaprolactone produced by zinc-guanidine complexes have favorably high crystallinities. In fact, the obtained polylactide shows a more robust degradation profile than its Sn(Oct)$_2$-catalysed equivalent due to a higher degree of crystallinity.*

Introduction

Biodegradable and sustainable polymers are key to solving the environmental problems of plastic waste and depletion of fossil resources as the common monomer source. Hence, the use of renewable resources needs to be combined with the synthesis of biodegradable and biocompatible polymers.[1] Monomers for these bioplastics already exist, for example, lactide (LA),[2] ε-caprolactone (ε-CL)[3] and γ-butyrolactone[4] are bio-based monomers.[5] Polylactide (PLA) is currently the most widely produced biodegradable bioplastic.[6] PLA is made from maize, sugar beets or other biomass by fermentation to lactic acid. Dimerization of lactic acid results in LA and a subsequent ring-opening polymerization (ROP) of LA, using a metal-catalyzed coordination-insertion mechanism, yields PLA.[2,7] The production of polycaprolactone (PCL) ensues via ROP of ε-CL, which can also be obtained from renewable raw materials: starting from C$_6$ sugars via 5-(hydroxymethyl)furfural and 1,6-hexanediol.[3b,8] This production method of ε-CL avoids the industrially used Baeyer–Villiger oxidation premised on petroleum-based cyclohexanone.[9]

Tin(II) bis(2-ethylhexanoate) [Sn(Oct)$_2$] combined with an alcohol as co-initiator is used industrially as catalyst to produce PLA and PCL.[7b,10] This catalyst has high activity in the ROP, leads to colorless polymer with high molar masses and maintains its high activity even at low catalyst concentrations. Even so, the accumulation of the catalyst in the environment is critical, since Sn(Oct)$_2$ is classified as toxic.[7b,10b] Furthermore, PLA is widely used in medical applications for example, as scaffold in regenerative medicine and for implants.[11] Thus, due to toxicity issues biocompatible metal complexes are sought as alternatives to Sn(Oct)$_2$. Several alternative metals such as zinc,[12] magnesium,[13,18] or iron[14] are known for the ROP for this purpose. Further, higher catalyst activity, low catalyst concentrations as well as a high tolerance to impurities and elevated temperatures would be ideal for any alternative complex.[15]

For the polymerization of PCL different zinc-based catalyst systems have been published. Dagorne et al. worked with a zinc alkyl catalyst[16] as well as with phosphinophenolate ligands[17] to polymerize ε-CL. However, these catalysts did not exhibit superior polymerization activity and did not produce long-chain polymers. As shown by Sánchez-Barba et al.[13a] and Kol and co-workers,[18] higher catalytic activities are achieved by using magnesium catalysts. While these catalysts indeed show high polymerisation activity and result in high molecular weight PCL, there sensitivity towards air and water still limits their large-scale application.

Most of the published zinc complexes in LA polymerization also show high activity, but they are usually sensitive to water, oxygen or impurities and are tested in solution, under non-industrial conditions.[12a,b,19] McKeown et al. polymerized LA under industrial conditions by using zinc Schiff base complexes.[12g] Also, dinuclear zinc Schiff base complexes showed activity in LA polymerization under solvent-free conditions.[20] Yet, the attained molar masses are not very high. A long known active and robust catalyst family for the ROP of LA are guanidine complexes, which have relevant properties for industrial use.[12c,e,21,25] In the last few years, very

[*] A. Hermann, Dr. A. Metz, J. Heck, Dr. A. Hoffmann,
Prof. Dr. S. Herres-Pawlis
Institute of Inorganic Chemistry, RWTH Aachen University
Landoltweg 1, 52074 Aachen (Germany)
E-mail: sonja.herres-pawlis@ac.rwth-aachen.de

Dr. S. Hill, Prof. Dr. L. Hartmann
Institute of Organic and Macromolecular Chemistry, Heinrich Heine University Düsseldorf
Universitätsstraße 1, 40225 Düsseldorf (Germany)
E-mail: laura.hartmann@hhu.de

Supporting information and the ORCID identification number(s) for the author(s) of this article can be found under:
https://doi.org/10.1002/anie.202008473.

active *N,O*-donor zinc guanidine complexes have been reported.[12d,22] However, the activity was slightly less compared to Sn(Oct)$_2$. Recently, an iron-carboxyguanidine complex was found to be the fastest catalyst for the ROP of LA in a solvent-free polymerization with higher catalytic activity than the industrially used Sn(Oct)$_2$.[14c]

Given the need towards more sustainable processes and materials with regard to a circular economy, the demand will definitely increase for polyesters like PCL and PLA.[23] Catalytic processes which can produce biodegradable polymers with specific properties and biocompatible profiles for high-value applications are thus very important.[24] Therefore, with the goal to replace the toxic industrially used catalyst, we designed a new robust *N,N*-donor zinc-guanidine complex as a sustainable alternative. It contains two bisguanidine ligands around the zinc ion which enhances the Lewis acidity and hence the ROP activity.[25] This complex exhibits the fastest known catalytic activity in bulk for the ROP of cyclic esters. Not only is this catalyst faster than all previously published robust and biocompatible catalysts for the LA polymerization, but it is also the very first guanidine complex that polymerizes LA in solution and it ensures higher crystallinity of the obtained polymer material, an important feature for various applications such as its use for medical implants.[26]

Crystallinity plays a vital role in determining a given polymer's application for example, highly crystalline PLA is relevant for biological applications with long-exposure times such as in bone regeneration.[26a] Therefore, catalyst choice is pertinent for generating the desired material properties, whilst avoiding additional post-production processing to yield a desired profile.[7c,27]

Results and Discussion

The zinc bis(chelate) complex [Zn{(*R,R*)-DMEG$_2$-(1,2)ch}$_2$](OTf)$_2$·THF (**1**) was synthesized in two-steps and fully characterized. Ligand (*R,R*)-DMEG$_2$(1,2)ch[12e] was reacted with zinc(II) trifluoromethylsulfonate to achieve complex **1**. The structure of complex **1** was determined by single-crystal X-ray diffraction (Figure 1). The zinc ion in **1** is four-coordinated by two bisguanidine chelate ligands in a distorted tetrahedral manner indicated by a τ_4 value of 0.62 and bite angles of 86.2(3)° and 86.5(3)° (crystallographic details, see Supporting Information).

We used TGA to examine the thermal stability of complex **1**, which shows stability at industrially relevant conditions for more than one hour (150°C and 200°C) (Figure S6). Therefore, an industrially relevant reaction temperature of 150°C was used to test complex **1** in the polymerization of LA as well as ε-CL in solvent-free conditions. The polymerizations were performed in a reactor monitored by in situ Raman spectroscopy. Various [M]/[I] ratios were investigated to determine the catalyst activity (Table S4). By linear regression of k_{app} against the used initiator concentration the rate constant of propagation k_p is obtained, allowing a comparison of different catalyst systems. The k_p value was determined for both polymerizations and compared with the industrial used catalyst Sn(Oct)$_2$.
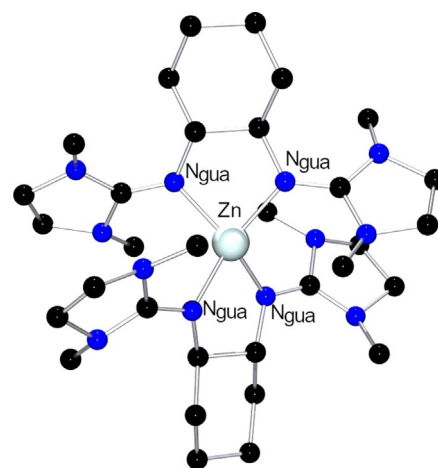

Figure 1. Molecular structure of the cation [Zn{(*R,R*)-DMEG$_2$-(1,2)ch}$_2$]$^{2+}$ in crystals of **1**. Hydrogen atoms are omitted for clarity.

Complex **1** is highly active for the ROP of non-purified technical *rac*-LA and ε-CL. The polymerization data of technical grade *rac*-LA show high conversion after short times despite decreasing catalyst concentration. Moreover, these polymerizations demonstrate the robustness relating to moisture, oxygen and impurities. For the determination of the rate constant k_p [M]/[I] ratios between 500:1 and 2500:1 were applied and lead to a linear regression with very good approximation (Figure 2). This indicates, in combination with the linear regression of k_{app}, a pseudo-first-order reaction kinetics, typical for a coordination insertion mechanism.[28]

Complex **1** exhibits a k_p value of $1.43 \pm 0.09 \, \mathrm{L\,mol^{-1}\,s^{-1}}$ (Figure 2) for the polymerization of technical grade *rac*-LA at reaction times between 3 min and 15 min. Consequently, complex **1** is almost three times as fast as the fastest robust iron-guanidine complex published hitherto for the ROP of LA under industrial conditions ($k_p = 0.554 \pm 0.02 \, \mathrm{L\,mol^{-1}\,s^{-1}}$).[14c] A comparison of complex **1** with the industrially used Sn(Oct)$_2$ results in a rate constant k_p increased by nearly one order of magnitude ($k_p =$
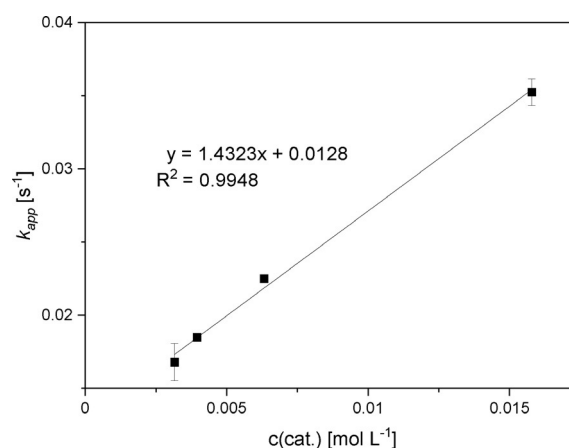

Figure 2. Plot of k_{app} against [**1**] with non-purified technical *rac*-LA for the determination of the propagation rate constant k_p. [M]/[I] = 500:1, 1250:1, 2000:1, 2500:1.

0.167 L mol⁻¹ s⁻¹).[12d] The resulting colorless and transparent polymers have high molar masses up to 100 000 g mol⁻¹, which is a common molecular weight used in various applications (such as packaging and medical applications).[11b]

In a further experiment, the catalyst concentration was decreased to reflect industrial conditions more accurately. By increasing the [M]/[I] ratio up to 5000:1 the catalyst activity decreased rapidly. After a short polymerization time of 5 min a stagnation was detected ceasing in a final conversion of 32% after 40 min. This can be explained by water and acid residues in the technical grade *rac*-LA which was used (Figure S11). To show that the low catalyst activity at a [M]/[I] ratio of 5000:1 is indeed due to the impurities of the non-purified technical grade LA the experiment was repeated with sublimated LA. After less than 4 min reaction time a conversion of 74% was achieved, which shows the restoration of the high activity (Figure S12). We investigated whether the catalyst is able to polymerize *rac*-LA selectively. The stereochemical properties of **1** may influence the tacticity of the resulting polymer. The polymer's tacticity was determined with a homonuclear decoupled ¹H NMR spectrum at a [M]/[I] ratio of 500:1 (Figure S13). The polymerization of *rac*-LA with complex **1** leads to an atactic polymer with $P_r = 0.55$ at 298 K.

Polymerization data of ε-CL similar to LA polymerization shows a linear progresion of the kinetics (Figure S14). The rate constant k_p of complex **1** in the ROP of ε-CL is determined for [M]/[I] ratios between 500:1 and 2500:1 (Figure 3). The resulting value of $k_p = 0.049 \pm 0.004$ L mol⁻¹ s⁻¹ is ca. 30 times smaller than the LA polymerization rate constant k_p. Under identical reaction conditions Sn(Oct)₂ polymerized ε-CL with a rate constant of $k_p = 0.0267 \pm 0.0034$ L mol⁻¹ s⁻¹. This shows that also the polymerization of ε-CL is twice as fast with **1** than with Sn(Oct)₂ as already observed for LA polymerization, giving access to colorless PCL with molar masses of 129 000 g mol⁻¹.

For both polymerizations (LA and ε-CL) end group analyses were carried out using MALDI-ToF-MS. This method allows the investigation of the initiation mechanism. Short-chain polymers need to be prepared for these analyses.
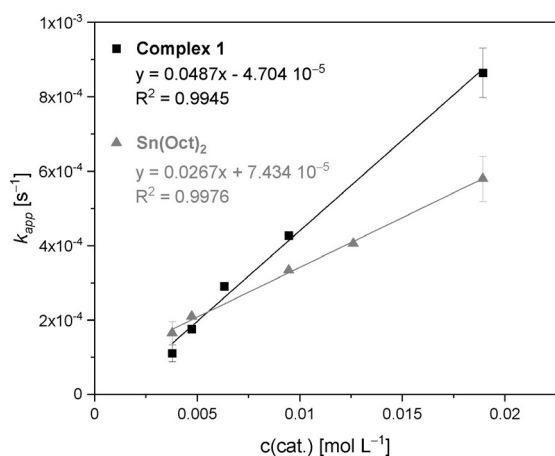
Due to the high reaction activity of complex **1** and the resulting high molar masses obtained within a short time, we prepared the samples with co-initiator leading to a reduced average molar mass through the additional larger number of initiated chains. Indeed, we observe end groups which can be assigned to the ligand and complex as well as a ligand binding a zinc ion, indicating the catalyst's characteristic being active as single-site catalyst (Figure S23/24).

Besides polymerization in bulk with high relevance for large-scale industrial production, the polymerization in solution is important to obtain high-performance materials for medical application. Complex **1** is the very first guanidine complex that polymerizes LA in solution. The high catalyst activity of complex **1** in the solvent-free ROP implies catalytic activity in a solution polymerization. First a THF solution was used, because it is an established solvent for the polymerization of LA.[12b,29] However, no conversion was observed after 24 h and a [M]/[I] ratio of 500:1 (Table S6). In contrast, the polymerization proceeded smoothly in toluene over a broad range of [M]/[I] ratios. The different [M]/[I] ratios enable the determination of the rate constant k_p for the solvent polymerization of recrystallized *L*-LA with complex **1** (Figure 4). The solution polymerization k_p value of 0.411 ± 0.04 L mol⁻¹ s⁻¹ is around three times smaller than LA polymerization in bulk. Colourless polymers with a molar mass of 40 000 g mol⁻¹ were obtained. To classify the activity of **1** a comparison with the fastest zinc catalyst for LA polymerization in solution is useful. This published catalyst resulted in an activity of $k_{app} = 0.029$ s⁻¹ ([M]/[I] = 1000:1, 25 °C, THF, 126 s, 97 %).[12b] Our catalyst results in a k_{app} of 5.24×10^{-4} s⁻¹ at the same [M]/[I] ratio, but withstands the higher temperature of 100 °C in toluene and the use of technical LA. Analogue experiments for Sn(Oct)₂ reveal a rate constant of 0.0143 ± 0.0012 L mol⁻¹ s⁻¹ and therefore that the rate constant of our complex **1** is around thirty times higher.

To more closely mimic industrial conditions and perform reactions at a temperature of 150 °C, diphenyl ether was tested as solvent, because of its high boiling point. The rate constant increased as expected for the higher temperature to

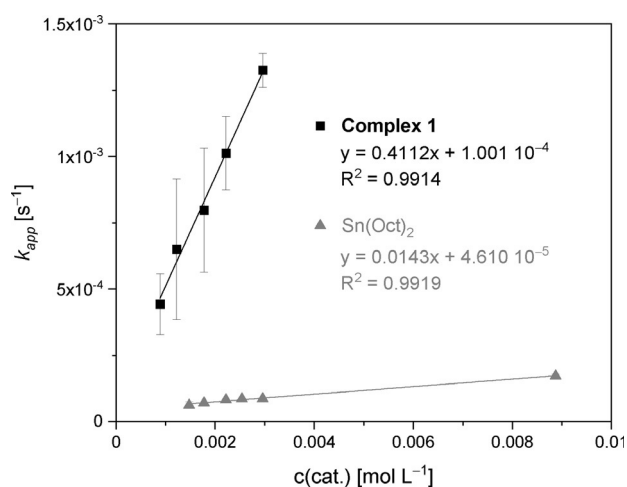***Figure 3.*** Plot of k_{app} against catalyst concentration with ε-CL for complex **1** and Sn(Oct)₂.

Figure 4. Plot of k_{app} against catalyst concentration with with recrystallized *L*-LA in toluene for complex **1** and Sn(Oct)₂.

a k_{app} value of 2.95×10^{-3} s^{-1} at a [M]/[I] ratios of 1000:1 (Figure S20).

To elucidate the origin of the high catalytic activity, density functional theory (DFT) studies were performed (for computational details see Supporting Information). Complex **1** was compared to a structurally related catalyst [Zn-{DMEG$_2$e}$_2$](OTf)$_2$, which was synthesised with an ethylene bridge instead of cyclohexane and showed a much lower activity for the polymerization of LA.[12c] It was found that complex **1** has a more distorted structure due to a higher steric requirement of the cyclohexane bridge compared to an ethylene bridging unit. Natural bond orbital (NBO) analyses[30] reveal that the donating lone-pairs (LP) of the guanidine groups have a different degree of overlap in both complexes: in complex **1**, the LP does not point directly to the zinc ion whereas in [Zn{DMEG$_2$e}$_2$](OTf)$_2$ the overlap is 5° better (Figure S5). This indicates that the ligands in **1** are not so tightly bound and might be easier replaced by an approaching LA molecule. Moreover, the NBO calculations provide charge-transfer energies for the dative interactions: in **1** those are calculated to 29.5 kcal mol^{-1}, in its ethylene congener to 33.0 kcal mol^{-1}. This underlines the weaker donor interactions of the same guanidine group in **1**. For further comparison, the related mono-chelate complex [Zn{(R,R)-DMEG$_2$(1,2)ch}Cl$_2$][12e] is considered: here, the ligand is the same but only one bisguanidine ligand coordinates to the zinc center. The observed ROP activity is considerably smaller with a k_{app} of 3.3×10^{-5} s^{-1} and polymerization reactions which needed hours instead of seconds. In this comparison, the NBO charges can be used to assess the Lewis acidity. In **1**, the zinc ion has a NBO charge of $+1.66 e^-$ whereas in [Zn{(R,R)-DMEG$_2$(1,2)ch}Cl$_2$] it amounts to $+1.55 e^-$. This difference is significant and correlates with the higher activity of **1** compared to its mono-chelate counterpart. Hence, both structural features—assembling four guanidine donors and geometric distortion around the zinc center—are key to the extraordinarily high ROP activity of **1**.

Having a closer look at the PCL and PLA materials obtained in this study, the properties of *L*-PLA, *rac*-PLA and PCL samples were investigated using gel permeation chromatography (GPC), NMR spectroscopy, and differential scanning calorimetry (DSC) (see Supporting Information for full details) specifically looking at molecular weight distributions as well as their characteristics as potentially semicrystalline materials (melting temperature, glass transition, degree of crystallinity).

Addressing PCL first, on average PCL samples catalyzed by either **1** or Sn(Oct)$_2$ (named **1**-PCL and Sn-PCL) showed similar molecular weights (M_n) above 130 000 g mol^{-1} and dispersities (*Đ*) of 1.7 (samples 1–6, Table S10). **1**-PCL and Sn-PCL exhibited identical NMR profiles (Figure S25) and DSC highlighted similar average melting temperatures ca. 56 °C, as well as similar degrees of crystallinity (X_c) of ca. 46 % akin to literature (samples 1–6, Table S11).[31]

Rac-LA-based PLA showed molecular masses of ca. 50 000 and 30 000 g mol^{-1} for **1** and Sn(Oct)$_2$ catalysts, respectively, (samples 15–16, see Table S10). In DSC analysis, *rac*-LA based samples derived from both catalysts showed no melting temperature up to 250 °C and thus are considered

amorphous materials. Analysis for PLA derived from *L*-LA showed average M_n values above 100 000 g mol^{-1} for both **1**- and Sn-PLA and *Đ* of 1.6 (samples 7–14, Table S10). Higher molecular weights in comparison to the *rac*-LA samples are likely due to the longer reaction time in the bulk polymerization set-up (see Table S10). Surprisingly, ^{1}H NMR highlighted differences between the methyl groups of **1**- and Sn-PLA, as Sn-PLA exhibited multiple, distinct chemical signals (Figure S26). Additional analysis by homonuclear decoupled experiments showed that **1**-PLA is isotactic PLA while Sn-PLA is atactic with a probability of racemic enchainment P_r of 0.28 (Figure S27). The methine region of **1**-PLA resulted in a single tetrad *iii* using homonuclear decoupled ^{1}H NMR spectroscopy (Figure S27 A-B) indicative for purely isotactic PLA. The homonuclear decoupled Sn-PLA spectra show a splitting of the main tetrad and three minor tetrads (Figure S27 D). The microstructure of Sn-PLA may be the result of epimerization which is suppressed by adding alcohol as co initiator as observed in commercially available PLA (Figure S28). Furthermore, DSC also revealed glass transition temperature (T_g) and X_c disparities for Sn-PLA and **1**-PLA (samples 7–14, Table S11): **1**-PLA exhibited a 58 °C T_g and 60 % X_c, whereas Sn-PLA recorded a lower T_g of 48 °C and X_c of 47 %, in line with precedent.[32] Thus, on average, **1**-PLA has ca. 15 % higher degree of crystallinity. Interestingly however, as both Sn- and **1**-PLA exhibited near-identical T_m values of 174 and 175 °C (Table S11, including also a comparison to a commercially available PLA sample), respectively, this indicates their crystalline domain character is equivalent irrespective of catalyst. A lower T_g and X_c for Sn-PLA suggests a higher level of disorder and inter-chain spacing, or free volume, in its amorphous domains.[33]

The content of **1** in the precipitated polymers was determined by atomic absorption spectroscopy (AAS) establishing the level of Zn present in PCL and PLA post-polymerization (see Supporting Information). It was found that Zn was present in both samples at 0.3 mg Zn per gram of polymer, a weight fraction of 0.03 % (Figure S29).

One of the key properties for a sustainable lifecycle of both, PCL and PLA, is their degradability.[34] It is well known that both PCL and PLA are degradable under various conditions, however, it has also been shown that degradation can be affected by different material parameters. Therefore, in order to study and compare the different polymers for their degradation profiles in dependence of the catalyst used during synthesis, a series of degradation experiments was performed. Experiments were conducted initially by immersing samples (pellet form) in MilliQ water at 70 °C for 24, 72 and 168 h (see Supporting Information). On average, under the conditions tested, Sn and **1**-PCL lost approximately 5–10 % mass (Figures 5 and S30). The amorphous *rac*-PLA samples both show ca. 10 % mass loss. Aliphatic polyester degradation is multifactorial but perhaps most critical is a polymer's degree of crystallinity X_c.[35] Accordingly, similar degradation profiles were expected since both PCL samples showed similar X_c. Thus, for PCL derived from either **1** or Sn-catalyst as well as for *rac*-PLA derived from the two catalyst, no difference in properties including degradation profiles was

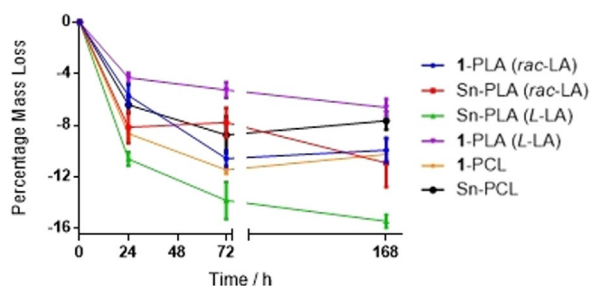| Polymer	M_n [kg mol^{-1}] [a]	$Đ$ [a]	X_c [%] [b]	Mass Loss [%] [c]
1-PCL	174	1.8	45 ± 1	9 ± 1
Sn-PCL	161	1.7	46 ± 2	6 ± 1
1-PLA (L)	127	1.5	60 ± 2	6 ± 1
Sn-PLA (L)	158	1.4	47 ± 6	17 ± 2
1-PLA (rac)	50	1.7	n.d.	10 ± 1
Sn-PLA (rac)	32	1.6	n.d.	11 ± 2

Figure 5. (Top) Macromolecular, crystallinity, and degradation properties of obtained polymers comparing Sn and Zn catalyst. (Bottom) Mass loss studies for selected samples (above Table) incubated at 70 °C in MilliQ water after 1, 3, and 7 days. [a] corresponds to samples 2, 6, 10, 13, 15, and 16 in Table S10; [b] average value of 3 (PCL) and 4 (PLA (L)) samples as determined by DSC (see Supporting Information), n.d. = not determined, samples are amorphous; [c] average percentage mass loss immersed in MilliQ H$_2$O, at 70 °C in 7d (see Supporting Information).

observed in dependence of the catalyst used during material preparation.

Clearly, however, different degradation behavior was observed when comparing Sn-PLA and 1-PLA derived from L-LA, with 1-PLA showing about 6 % mass loss, and Sn-PLA a higher mass loss of ca. 17 % (Figures 5 and S30). This is entirely consistent with the observed differences in X_c and T_g for these two PLA samples, where Sn-PLA with its lower X_c and T_g, and likely higher free volume in the amorphous, hydrolysis-prone domains, shows higher mass loss. Additional biological and environmental conditions were tested on selected PLA samples to further investigate degradation profiles (see Supporting Information). Polymer samples were immersed in a variety of aqueous media (MilliQ or tap water, phosphate-buffered saline (PBS) or 1 M HCl solution) and incubated at 37 °C for either 24, 72 or 168 h (see Supporting Information). Additionally, samples incubated at 37 °C and dissolved in an esterase-containing PBS solution effectively mimicked physiological conditions (see Supporting Information). Under all conditions tested 1-PLA showed universal 5–10 % mass loss, whereas Sn-PLA showed consistently higher mass losses of ca. 20 % (Figures S31-33), congruous with expectations. Environmental testing is paramount too, as the ultimate destination of a polymer is unknown but probable routes are to landfill, or as detritus in the environment and water course.[36] To ascertain "real world" mass losses samples were immersed in pond water or soil followed by environmental exposure for 7 or 14 days (see Supporting Information and Figure S34). 1-PLA lost 5–10 % mass in both pond water and soil after 14 days, whereas Sn-PLA had 25 % and 17 % mass loss in pond water and soil, respectively (Figures S35/36).

Under biological, physiological and environmental triggers the degradation discrepancy between 1- and Sn-PLA is evident, confirming the correlation between crystallinity content, amorphous domain polymer mobility, and hydrolytic degradation. Further studies of longer degradation periods, of months to years, are ongoing to gain further insight into the likely interplay of catalyst choice, polymer properties, and degradation profile.

The advantage of complex 1 is clear when aiming for high stability PLA with higher crystallinity, but at this point we cannot yet explain the underlying mechanism leading to high PLA X_c when using 1. It is known that catalysts, like Sn(Oct)$_2$, can produce multiple initiation species and thus heterogeneous chemical environments during polymerization.[37] Whether 1 can generate polymer chains with greater chemical homogeneity, favoring optimal chain packing into highly crystalline domains, ideal for long-exposure applications such as in medical implants,[38] is not known yet. This has to be further examined for example, X-ray crystallography or in situ small angle X-ray scattering,[39] however, this too will be part of future studies.

Conclusion

In conclusion, the presented zinc bisguanidine complex 1 shows a very high activity in the polymerization of the biogenic cyclic monomers LA and ε-CL. The catalyst's polymerization rate constant k_p is nearly one order of magnitude increased compared to the industrial used Sn-(Oct)$_2$ to 1.43 L mol^{-1} s^{-1} making 1 the fastest robust ROP catalyst. Complex 1 yields PLA and PCL with high conversion and high molar masses in a controlled manner under industrial polymerization conditions. Also a solution polymerization is possible with this catalyst, opening the doors for this type of polymerization in conjuction with robust guanidine complexes. Furthermore, studies established that complex 1 mediates the polymerisation to highly crystalline PCL and PLA, with significantly higher crystalline content and thus hydrolytic stability in case of L-LA than material produced with Sn(Oct)$_2$. This paves the way towards using the non-toxic 1-catalysed polymers for long-exposure bioapplications such as medical implants.

Acknowledgements

Conflict of interest

The authors declare no conflict of interest.

Keywords: bioplastic · crystallinity · polylactide · ring-opening polymerization · zinc

[1] a) J. R. Jambeck, R. Geyer, C. Wilcox, T. R. Siegler, M. Perryman, A. Andrady, R. Narayan, K. L. Law, *Science* **2015**, *347*, 768–771; b) Y. Zhu, C. Romain, C. K. Williams, *Nature* **2016**, *540*, 354; c) A. J. Ragauskas, C. K. Williams, B. H. Davison, G. Britovsek, J. Cairney, C. A. Eckert, W. J. Frederick, J. P. Hallett, D. J. Leak, C. L. Liotta, J. R. Mielenz, R. Murphy, R. Templer, T. Tschaplinski, *Science* **2006**, *311*, 484–489.

[2] R. A. Auras, L.-T. Lim, S. E. Selke, H. Tsuji, *Poly (lactic acid): synthesis, structures, properties, processing, and applications*, Wiley, Hoboken, **2011**.

[3] a) A. A. Rosatella, S. P. Simeonov, R. F. M. Frade, C. A. M. Afonso, *Green Chem.* **2011**, *13*, 754–793; b) T. Buntara, S. Noel, P. H. Phua, I. Melián-Cabrera, J. G. de Vries, H. J. Heeres, *Angew. Chem. Int. Ed.* **2011**, *50*, 7083–7087; *Angew. Chem.* **2011**, *123*, 7221–7225.

[4] G. Budroni, A. Corma, *J. Catal.* **2008**, *257*, 403–408.

[5] G. L. Gregory, E. M. López-Vidal, A. Buchard, *Chem. Commun.* **2017**, *53*, 2198–2217.

[6] *Global production capacties of bioplastics, European Bioplastics*, https://www.european-bioplastics.org/market/. 11.10.2019.

[7] a) *Handbook of Ring-Opening Polymerization*, Wiley-VCH, Weinheim,, **2009**; b) H. R. Kricheldorf, *Chemosphere* **2001**, *43*, 49–54; c) S. Farah, D. G. Anderson, R. Langer, *Adv. Drug Delivery Rev.* **2016**, *107*, 367–392.

[8] V. Thaore, D. Chadwick, N. Shah, *Chem. Eng. Res. Des.* **2018**, *135*, 140–152.

[9] M. C. Rocca, G. Carr, A. B. Lambert, D. J. MacQuarrie, J. H. Clark, in *US Pat.*, Solvay SA, **2003**, US6531615B2.

[10] a) M. Labet, W. Thielemans, *Chem. Soc. Rev.* **2009**, *38*, 3484–3504; b) A. Stjerndahl, A. Finne-Wistrand, A.-C. Albertsson, C. M. Bäckesjö, U. Lindgren, *J. Biomed. Mater. Res. Part A* **2008**, *87*, 1086–1091.

[11] a) A. J. R. Lasprilla, G. A. R. Martinez, B. H. Lunelli, A. L. Jardini, R. M. Filho, *Biotechnol. Adv.* **2012**, *30*, 321–328; b) E. Castro-Aguirre, F. Iñiguez-Franco, H. Samsudin, X. Fang, R. Auras, *Adv. Drug Delivery Rev.* **2016**, *107*, 333–366; c) M. A. Ghalia, Y. Dahman, *J. Polym. Res.* **2017**, *24*, 74.

[12] a) C. K. Williams, L. E. Breyfogle, S. K. Choi, W. Nam, V. G. Young, M. A. Hillmyer, W. B. Tolman, *J. Am. Chem. Soc.* **2003**, *125*, 11350–11359; b) A. Thevenon, C. Romain, M. S. Bennington, A. J. P. White, H. J. Davidson, S. Brooker, C. K. Williams, *Angew. Chem. Int. Ed.* **2016**, *55*, 8680–8685; *Angew. Chem.* **2016**, *128*, 8822–8827; c) J. Börner, S. Herres-Pawlis, U. Flörke, K. Huber, *Eur. J. Inorg. Chem.* **2007**, 5645–5651; d) P. M. Schäfer, P. McKeown, M. Fuchs, R. D. Rittinghaus, A. Hermann, J. Henkel, S. Seidel, C. Roitzheim, A. N. Ksiazkiewicz, A. Hoffmann, A. Pich, M. D. Jones, S. Herres-Pawlis, *Dalton Trans.* **2019**, *48*, 6071–6082; e) A. Metz, P. McKeown, B. Esser, C. Gohlke, K. Kröckert, L. Laurini, M. Scheckenbach, S. N. McCormick, M. Oswald, A. Hoffmann, M. D. Jones, S. Herres-Pawlis, *Eur. J. Inorg. Chem.* **2017**, 5557–5570; f) M. Fuchs, S. Schmitz, P. M. Schäfer, T. Secker, A. Metz, A. N. Ksiazkiewicz, A. Pich, P. Kögerler, K. Y. Monakhov, S. Herres-Pawlis, *Eur. Polym. J.* **2020**, *11*, 2381–2389; g) P. McKeown, S. N. McCormick, M. F. Mahon, M. D. Jones, *Polym. Chem.* **2018**, *9*, 5339–5347; h) J. Payne, P. McKeown, M. F. Mahon, E. A. C. Emanuelsson, M. D. Jones, *Polym. Chem.* **2020**, *165*, 170–181.

[13] a) L. F. Sánchez-Barba, A. Garcés, M. Fajardo, C. Alonso-Moreno, J. Fernández-Baeza, A. Otero, A. Antiñolo, J. Tejeda, A. Lara-Sánchez, M. I. López-Solera, *Organometallics* **2007**, *26*, 6403–6411; b) B. J. Ireland, C. A. Wheaton, P. G. Hayes, *Organometallics* **2010**, *29*, 1079–1084; c) L. Wang, H. Ma, *Macromolecules* **2010**, *43*, 6535–6537.

[14] a) U. Herber, K. Hegner, D. Wolters, R. Siris, K. Wrobel, A. Hoffmann, C. Lochenie, B. Weber, D. Kuckling, S. Herres-Pawlis, *Eur. J. Inorg. Chem.* **2017**, 1341–1354; b) R. Duan, C. Hu, X. Li, X. Pang, Z. Sun, X. Chen, X. Wang, *Macromolecules* **2017**, *50*, 9188–9195; c) R. D. Rittinghaus, P. M. Schäfer, P. Albrecht, C. Conrads, A. Hoffmann, A. N. Ksiazkiewicz, O. Bienemann, A. Pich, S. Herres-Pawlis, *ChemSusChem* **2019**, *12*, 2161–2165.

[15] Z. Zhong, P. J. Dijkstra, J. Feijen, *Angew. Chem. Int. Ed.* **2002**, *41*, 4510–4513; *Angew. Chem.* **2002**, *114*, 4692–4695.

[16] C. Romain, V. Rosa, C. Fliedel, F. Bier, F. Hild, R. Welter, S. Dagorne, T. Avilés, *Dalton Trans.* **2012**, *41*, 3377–3379.

[17] C. Fliedel, V. Rosa, F. M. Alves, A. M. Martins, T. Avilés, S. Dagorne, *Dalton Trans.* **2015**, *44*, 12376–12387.

[18] T. Rosen, I. Goldberg, W. Navarra, V. Venditto, M. Kol, *Angew. Chem. Int. Ed.* **2018**, *57*, 7191–7195; *Angew. Chem.* **2018**, *130*, 7309–7313.

[19] a) T. Rosen, Y. Popowski, I. Goldberg, M. Kol, *Chem. Eur. J.* **2016**, *22*, 11533–11536; b) B. M. Chamberlain, M. Cheng, D. R. Moore, T. M. Ovitt, E. B. Lobkovsky, G. W. Coates, *J. Am. Chem. Soc.* **2001**, *123*, 3229–3238; c) A. J. Nijenhuis, D. W. Grijpma, A. J. Pennings, *Macromolecules* **1992**, *25*, 6419–6424.

[20] P. M. Schäfer, K. Dankhoff, M. Rothemund, A. N. Ksiazkiewicz, A. Pich, R. Schobert, B. Weber, S. Herres-Pawlis, *ChemistryOpen* **2019**, *8*, 1020–1026.

[21] a) J. Börner, I. dos Santos Vieira, A. Pawlis, A. Döring, D. Kuckling, S. Herres-Pawlis, *Chem. Eur. J.* **2011**, *17*, 4507–4512; b) P. M. Schäfer, S. Herres-Pawlis, *ChemPlusChem* **2020**, *85*, 1044–1052.

[22] P. M. Schäfer, M. Fuchs, A. Ohligschläger, R. Rittinghaus, P. McKeown, E. Akin, M. Schmidt, A. Hoffmann, M. A. Liauw, M. D. Jones, S. Herres-Pawlis, *ChemSusChem* **2017**, *10*, 3547–3556.

[23] D. Maga, M. Hiebel, N. Thonemann, *Resour. Conserv. Recycl.* **2019**, *149*, 86–96.

[24] a) M. Hong, E. Y. X. Chen, *Green Chem.* **2017**, *19*, 3692–3706; b) X. Tang, E. Y. X. Chen, *Chem* **2019**, *5*, 284–312.

[25] J. Börner, U. Flörke, K. Huber, A. Döring, D. Kuckling, S. Herres-Pawlis, *Chem. Eur. J.* **2009**, *15*, 2362–2376.

[26] a) G. Narayanan, V. N. Vernekar, E. L. Kuyinu, C. T. Laurencin, *Adv. Drug Delivery Rev.* **2016**, *107*, 247–276; b) A. Kashirina, Y. Yao, Y. Liu, J. Leng, *Biomater. Sci.* **2019**, *7*, 3961–3983.

[27] a) R. E. Drumright, P. R. Gruber, D. E. Henton, *Adv. Mater.* **2000**, *12*, 1841–1846; b) S. Lambert, M. Wagner, *Chem. Soc. Rev.* **2017**, *46*, 6855–6871.

[28] P. W. Atkins, J. De Paula, J. Keeler, *Atkins' physical chemistry*, Oxford university press, Oxford, **2018**.

[29] D. Myers, A. J. P. White, C. M. Forsyth, M. Bown, C. K. Williams, *Angew. Chem. Int. Ed.* **2017**, *56*, 5277–5282; *Angew. Chem.* **2017**, *129*, 5361–5366.

[30] a) E. Glendening, J. Badenhoop, A. Reed, J. Carpenter, J. Bohmann, C. Morales, C. Landis, F. Weinhold, *Theoretical Chemistry Institute, University of Wisconsin, Madison, WI* **2013**, available at: https://nbo6.chem.wisc.edu/, accessed Feb. 1, 2013; b) E. D. Glendening, C. R. Landis, F. Weinhold, *J. Comput. Chem.* **2013**, *34*, 1429–1437.

[31] M. J. Jenkins, K. L. Harrison, *Polym. Adv. Technol.* **2008**, *19*, 1901–1906.

[32] a) C. Liu, Y. Jia, A. He, *Int. J. Polym. Sci.* **2013**, *2013*, 315917; b) R. Suuronen, T. Pohjonen, J. Hietanen, C. Lindqvist, *J. Oral Maxil. Surg.* **1998**, *56*, 604–614.

[33] R. P. White, J. E. G. Lipson, *Macromolecules* **2016**, *49*, 3987–4007.

[34] J. Payne, P. McKeown, M. D. Jones, *Polym. Degrad. Stab.* **2019**, *165*, 170–181.

[35] L. N. Woodard, M. A. Grunlan, *ACS Macro Lett.* **2018**, *7*, 976–982.

[36] R. Geyer, J. R. Jambeck, K. L. Law, *Sci. Adv.* **2017**, *3*, e1700782.

[37] a) P. J. Dijkstra, H. Du, J. Feijen, *Polym. Chem.* **2011**, *2*, 520–527; b) M. Ryner, K. Stridsberg, A.-C. Albertsson, H. von Schenck, M. Svensson, *Macromolecules* **2001**, *34*, 3877–3881.

[38] A. Majola, S. Vainionpää, K. Vihtonen, J. Vasenius, P. Törmälä, P. Rokkanen, *Int. Orthop.* **1992**, *16*, 101–108.

[39] B. Chu, B. S. Hsiao, *Chem. Rev.* **2001**, *101*, 1727–1762.